RSC Advances

PAPER

View Article Online
View Journal | View Issue



Cite this: *RSC Adv.*, 2015, **5**, 27197

# Aggregation behaviours and bactericidal activities of novel cationic surfactants functionalized with amides and ether groups†

Guangzhou Cao,[a] Xiangfeng Guo,*[a] Lihua Jia*[b] and Xuhua Tian[b]

Received 16th November 2014
Accepted 9th March 2015

DOI: 10.1039/c4ra14645j

www.rsc.org/advances

A series of novel cationic surfactants, *N*-alkylcaramoylmethyl-*N*-[2-(2-phenoxyacetamido)-ethyl]-*N*,*N*-dimethylammonium chloride, were synthesized and their chemical structures were characterized using $^{1}$H-NMR, $^{13}$C-NMR, ESI-MS and FT-IR. Their aggregation behaviours in aqueous solution were systematically investigated by surface tension and electrical conductivity methods. It was found that the surfactants have higher surface activity compared with a similar structural surfactant. A series of thermodynamic parameters of aggregation indicate that the aggregation is entropy-driven at the investigated temperatures. In addition, they possess excellent bactericidal activities against the selected strains.

## Introduction

Cationic surfactants are widely applied in germicides,[1–3] emulsification,[4] foaming,[5] detergent,[6] drug delivery[7,8] and materials synthesis,[9,10] *et al.* Recently, quaternary ammonium surfactants containing amide, ether, or other functional groups have been extensively studied due to several interesting properties such as low-toxicity or biodegradability.[11–13] It was found that the surfactants with amide functionalization could enhance the aggregation ability compared with those without an amide group, and the aggregation properties depend strongly on the position and number of amide bonds.[14] Morpholinium-based amide-functionalized ionic liquids (ILs) in aqueous medium showed better surface activity and much lower critical micellar concentration (CMC) compared to non-functionalized ILs, which was assigned to the intermolecular H-bonding for the presence of the amide group along with the relatively greater hydrophobicity and larger size of the morpholinium headgroup.[15] Ether functionalized pyridinium cationic surfactants displayed lower CMC values compared with that of conventional cationic surfactants without ether bond.[16] Bis-(*N*-(3-alkylamidopropyl)-*N*,*N*-dimethyl)-*p*-phenylene diammonium dichloride[17] at the air–water interface showed higher surface activity, which resulted from the intramolecules hydrogen bond originated from the amide group of long alkyl chain, and the micellization process is entropy-driven at the investigated temperatures. The high surface activity of 1-(alkylcaramoylmethyl)-pyridinium chloride is correlated directly with the intermolecular H-bonding for the presence of the amide group,[18] and the micellization process is entropy-driven process in the investigated temperatures. The micellar properties of benzyl-(2-acylaminoethyl)-dimethyl-ammonium chloride were explained for the formation of direct- or water-mediated hydrogen bonding between the amide groups, plus hydrophobic interactions between its benzyl and the alkyl groups.[19]

It is well known that *N*-dodecyl-*N*-benzyl-*N*,*N*-dimethyl ammonium chloride (1227) is a conventional cationic surfactants, and widely used as bactericide.[20] However, it has relatively high CMC, and the microorganism had the drug-resistance to 1227 for it has been used for a long-term as medical disinfectants.[21] The bactericidal performance of cationic surfactants with amide and ether functional groups based on phenol still received little attention.

Herein, we designed and synthesized a series of cationic surfactants with amide and ether functional groups, namely *N*-alkylcaramoylmethyl-*N*-[2-(2-phenoxyacetamido)-ethyl]-*N*,*N*-dimethylammonium chloride ($C_n$PDA, $n = 12, 14, 16$), and their aggregation behaviours were investigated by using the measurements of surface tension and conductivity, and compared with that of the similar structural surfactants. The relationships of the aggregation and the structure were discussed. The bacterial activities were determined and compared with that of 1227, which may serve for potential application as a new sterilizing agent in the future.

## Results and discussion

### Surface properties of $C_n$PDA

Surface tension measurements were performed to determine surface behaviour and CMC of $C_n$PDA in aqueous solutions. The surface tension *versus* logarithm of concentration at 298.2 K was shown in Fig. 1.

[a]*Key Laboratory of Fine Chemicals of College of Heilongjiang Province, Qiqihar University, Qiqihar 161006, China. E-mail: xfguo@163.com*

[b]*College of Chemistry and Chemical Engineering, Qiqihar University, Qiqihar 161006, China. E-mail: jlh29@163.com*

† Electronic supplementary information (ESI) available. See DOI: 10.1039/c4ra14645j

As shown in Fig. 1, the surface tension decreases sharply with increasing concentration and attains a break point in the region of low surfactant concentrations. The surfactant concentration to the break point is assumed to be CMC of each surfactant. Surface tension method can not only estimate the CMC values of amphiphilic compounds, but also provide valuable information about the adsorption characteristics at the air–water interface. So, the saturation adsorption ($\Gamma$) and minimum area ($A_{\min}$) occupied per surfactant molecule at the air–water interface were analysed. According to the surface tension curves, $\Gamma$ can be calculated from the Gibbs eqn (1):

$$\Gamma = -\frac{1}{2.303nRT}\left(\frac{\partial\gamma}{\partial \log C}\right)_T \quad (1)$$

where $R$ is the gas constant; $T$ is the absolute temperature; $C$ is the surfactant concentration; $\gamma$ is the surface tension in mN $m^{-1}$; $\Gamma$ is the saturation adsorbed amount in μmol $m^{-2}$; $n$ is the number of ions that originate in solution by dissociation of the surfactant and whose concentration changes at the surface with the change of the bulk solution concentration, for a non-ionic surfactant, $n = 1$; for an ionic surfactant where the surfactant ion and the counterion are univalent, $n = 2$;[22] $n$ is taken as 2 in this paper. Gibbs equation has been generally used for calculation $\Gamma$ and $A_{\min}$ values, but the limitation for the calculation of area per molecule of surfactant through Gibbs adsorption equation has been questioned by various researchers,[23–25] for the presence of very small amount of impurities in cationic surfactants in recent reports. Thomas *et al.*[26] suggested that the only solution to this problem is to find a good model for activity behaviour in sub-micellar region. However, there is not a minimum near the breaking point, indicating that the surface chemical impurities could be ignored in this case. Nevertheless, the best way to verify the purity of samples is to employ other techniques such as neutron reflection.[26,27]

The minimum area occupied by each $C_n$PDA molecule ($A_{\min}$) at air–water interface was evaluated by the eqn (2):

$$A_{\min} = \frac{1}{\Gamma N_A} \quad (2)$$

where $N_A$ is Avogadro's number and $A_{\min}$ is in $nm^2$. The value of $\Gamma$ and $A_{\min}$ are listed in Table 1. It can be found the $\gamma_{CMC}$ of $C_n$PDA are smaller than that of $C_n$ABzMe$_2$Cl,[19] indicating that the surface activity of $C_n$PDA is superior to that of $C_n$ABzMe$_2$Cl. $\Gamma$ and $A_{\min}$ can reflect the molecule arrangement of surfactants at the air–water interface. The value of $A_{\min}$ for $C_{12}$PDA is slightly larger than that of $C_{12}$ABzMe$_2$Cl, meaning the arrangement of $C_{12}$PDA molecules is relatively looser compared with that of $C_{12}$ABzMe$_2$Cl at the air–water interface.

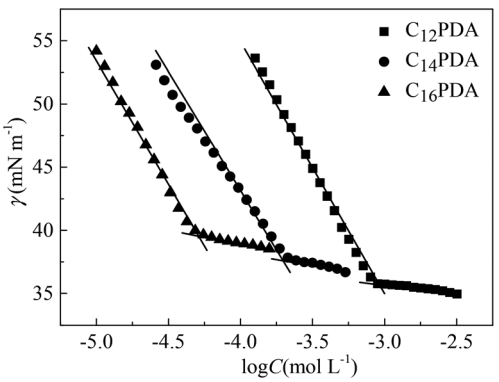


Fig. 1 Curves on surface tension *versus* log concentration of $C_n$PDA in aqueous solution.

Moreover, the CMC values are smaller than that of $C_n$ABzMe$_2$Cl with the same alkyl length (Table 1). The main difference in the structures between $C_n$PDA and $C_n$ABzMe$_2$Cl is that $C_n$PDA contains two amide groups and one ether group, while $C_n$ABzMe$_2$Cl only contains one amide group. The introduction of one ether and two amides groups increased the hydrophilicity, as well as promoted the hydrophobicity due to the hydrogen bonds of the inter-molecules and intra-molecule. It can be conclude for $C_n$PDA that the contribution of the hydrophobicity is stronger than the hydrophilicity by the two amides and one ether groups to the formation of micelles.[14,18]

The adsorption efficiency can be characterized by the value of logarithm of the surfactant concentration $C_{20}$ at which the surface tension of water is reduced by 20 mN $m^{-1}$ ($pC_{20}$). The larger the $pC_{20}$ value, the greater the tendency of the surfactant to adsorb at the air–water interface.[28,29] The values of $pC_{20}$ show an increasing tendency with increasing the length of hydrocarbon chain, which are 3.9, 4.6 and 4.9, respectively (Table 1). The $pC_{20}$ values of $C_n$PDA are somewhat larger than that of $C_n$ABzMe$_2$Cl with the same alkyl chain length.[19] It discloses that the adsorption efficiency of $C_n$PDA is stronger than that of $C_n$ABzMe$_2$Cl at the air–water interface.

For a homologous series of amphiphiles, CMC follows the empirical Stauff–Klevens rule, which accords with the following eqn (3):[30]

$$\log \mathrm{CMC} = A - BN \quad (3)$$

where CMC is the critical micelle concentration of $C_n$PDA; $N$ is the number of carbon atoms of the hydrophobic chains; A and B are empirical constants reflecting the free energy changes involved in transferring the hydrophilic group and a methylene unit of hydrophobic group from the aqueous phase to the micelle phase.[31] The effect of the hydrophobic chain lengths of $C_n$PDA and $C_n$ABzMe$_2$Cl on their CMC values at 298.2 K are shown in Fig. 2.

These plots exhibit a linear decrease in the CMC with the increase of hydrophobic chain length. The $B$ values of $C_n$PDA and $C_n$ABzMe$_2$Cl are 0.308 and 0.333, respectively, which are both close to 0.3 of conventional ionic surfactants.[31] Whereas the value of $A$ of $C_n$PDA is smaller than that of $C_n$ABzMe$_2$Cl, indicating that the ability to form micelles of $C_n$PDA is superior to that of $C_n$ABzMe$_2$Cl in aqueous solutions. It may result from that the hydrogen bonds of the inter-molecules and intra-molecule by the two amides and one ether groups, and the phenyl group at the end of larger hydrophilic group of $C_n$PDA may fold back toward the micellar core. Both of them have beneficial effect on the formation of micelles of $C_n$PDA.

## Thermodynamic of micellization

In order to investigate the aggregation behaviours of $C_n$PDA in aqueous solutions, the electrical conductivity ($\lambda$) was measured

 

Table 1 Surface properties of $C_n$PDA determined by surface tension in aqueous solution at 298.2 K

| | CMC (mmol $L^{-1}$) | $\gamma_{CMC}$ (mN $m^{-1}$) | $pC_{20}$ | $\Gamma$ (mmol $m^{-2}$) | $A_{min}$ ($nm^2$) |
|---|---|---|---|---|---|
| $C_{12}$PDA | 0.815 ± 0.045 | 35.8 ± 0.1 | 3.9 ± 0.2 | 1.92 ± 0.02 | 0.86 ± 0.01 |
| $C_{14}$PDA | 0.206 ± 0.014 | 37.8 ± 0.1 | 4.6 ± 0.2 | 1.45 ± 0.02 | 1.14 ± 0.02 |
| $C_{16}$PDA | 0.0461 ± 0.0029 | 39.8 ± 0.1 | 4.9 ± 0.2 | 1.88 ± 0.03 | 0.88 ± 0.02 |
| $C_{12}ABzMe_2Cl$[19] | 5.8 | 39.6 | 0.20 | 2.02 | 0.82 |
| $C_{14}ABzMe_2Cl$[19] | 1.3 | 39.9 | 0.39 | 2.10 | 0.79 |
| $C_{16}ABzMe_2Cl$[19] | 0.27 | 42.2 | 0.95 | 2.27 | 0.73 |

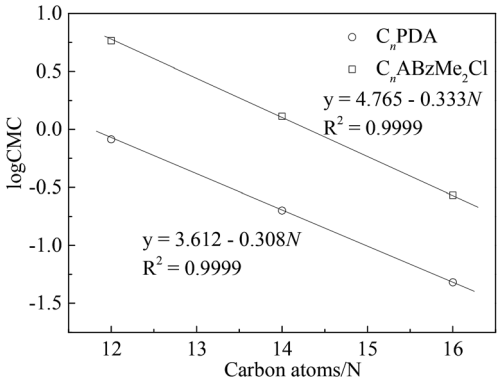


Fig. 2 Relationship between log CMC and the hydrocarbon chain length of $C_n$PDA at 298.2 K.

at 298.2, 303.2, 308.2, 313.2 and 318.2 K, respectively, as plotted in Fig. 3. There are two linear fragments in the typical curve, and the steep change of the slope is assigned to the CMC of $C_n$PDA. As shown in Table 2, the CMC values determined from the conductivity measurements were close to that of derived from surface tension at 298.2 K. Plots of CMC *versus* hydrocarbon chain length for $C_n$PDA at various temperatures are shown in Fig. 4. It can be seen the CMC values of $C_n$PDA increase slightly with the rise of temperature. In the first place, the hydration degree of the ionic headgroup domain decreases with a rise of temperature, which leads to an increasing hydrophobicity of the surfactant. Moreover, with an increasing temperature the breakdown of the structured water surrounding the hydrophobic domain can occur. This is unfavourable to surfactant aggregation, as the low entropy of the structured water is the key driving force of the self-association process.[32]

A comprehension of the specific binding of counterions to micelles is a prerequisite for an understanding of micellization of all kinds of aggregation in aqueous solutions. The degrees of dissociation ($\alpha$) of $C_n$PDA micelles in water were obtained using Evans' eqn (4), which considers that the mobility of micelles is nonzero.[33]

$$1000S_2 = \left(\frac{\alpha^2}{N_{agg}^{-\frac{2}{3}}}\right)(1000S_1 - \lambda_{Cl^-}) + \alpha\lambda_{Cl^-} \quad (4)$$

where $S_1$ and $S_2$ are the values of $\Delta\lambda/\Delta C$ below and above the CMC, respectively; $\lambda_{Cl^-}$ is the equivalent conductivity of the chloride ion at infinite dilution, the values of $\lambda_{Cl^-}$ derived from the literature;[34] the values of $N_{agg}$ were determined by steady-state fluorescence measurements (Table 2). The relationship of the degree of counterion binding ($\beta$) to micelles and $\alpha$ is as eqn (5):

$$\beta = 1 - \alpha \quad (5)$$

The values are listed in Table 2. In the present systems of $C_n$PDA (Fig. 5), $\beta$ decreases with the increase of the investigated temperature for $C_n$PDA. For an increase of the temperature can speed the thermal motion of the ions and molecules, which makes the counterions dissociate easier from the electrostatic bondage of the micelles,[35,36] in other words, the micelle becomes loose. The loose micelle structure decreases the adsorption ability to counterions and induces the smaller $\beta$ value.[32]

In addition, $\beta$ decreases with the aggregates as alkyl chain length increases also suggests that counter ions bind loosely.[37] Similar observations have been made in the case of conventional ammonium-cationic surfactants, where an increase in the alkyl

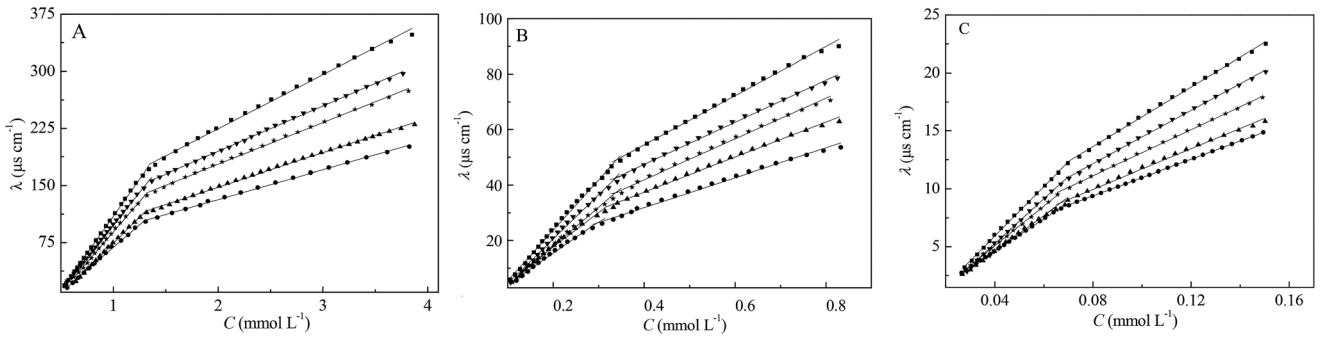


Fig. 3 Plots of specific conductivity *versus* the concentration of $C_{12}$PDA (A), $C_{14}$PDA (B) and $C_{16}$PDA (C) aqueous solution at different temperatures (●298.2 K, ▲303.2 K, ★308.2 K, ■313.2 K, ▼318.2 K).

Table 2 Values of CMC, $\beta$ determined by electrical conductivity measurement and $N_{agg}$ derived from steady-state fluorescence quenching measurements of $C_n$PDA

| | | 298.2 ± 0.1 K | 303.2 ± 0.1 K | 308.2 ± 0.1 K | 313.2 ± 0.1 K | 318.2 ± 0.1 K |
|---|---|---|---|---|---|---|
| $C_{12}$PDA | CMC (mmol $L^{-1}$) | 1.30 ± 0.02 | 1.31 ± 0.02 | 1.32 ± 0.02 | 1.33 ± 0.02 | 1.35 ± 0.02 |
| | $\beta$ | 0.855 ± 0.017 | 0.854 ± 0.017 | 0.850 ± 0.017 | 0.847 ± 0.016 | 0.841 ± 0.016 |
| | $N_{agg}$ | 67 ± 6 | 62 ± 6 | 60 ± 6 | 58 ± 5 | 55 ± 5 |
| $C_{14}$PDA | CMC (mmol $L^{-1}$) | 0.318 ± 0.006 | 0.320 ± 0.006 | 0.323 ± 0.006 | 0.328 ± 0.006 | 0.333 ± 0.006 |
| | $\beta$ | 0.771 ± 0.015 | 0.768 ± 0.015 | 0.765 ± 0.015 | 0.760 ± 0.015 | 0.753 ± 0.015 |
| | $N_{agg}$ | 36 ± 2 | 35 ± 2 | 34 ± 2 | 33 ± 2 | 31 ± 2 |
| $C_{16}$PDA | CMC (mmol $L^{-1}$) | 0.0650 ± 0.0013 | 0.0669 ± 0.0013 | 0.0678 ± 0.0013 | 0.0685 ± 0.0013 | 0.0712 ± 0.0014 |
| | $\beta$ | 0.683 ± 0.013 | 0.682 ± 0.013 | 0.677 ± 0.013 | 0.668 ± 0.013 | 0.664 ± 0.013 |
| | $N_{agg}$ | 10 ± 1 | 10 ± 1 | 10 ± 1 | 9 ± 1 | 9 ± 1 |

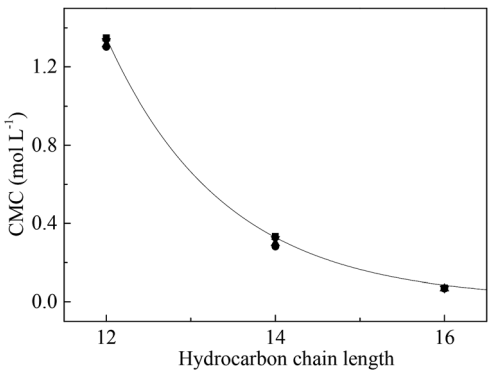


Fig. 4 Plots of CMC *versus* hydrocarbon chain length of $C_n$PDA at 298.2 K (●), 303.2 K (▲), 308.2 K (★), 313.2 K (■) and 318.2 K (▼).

chain length leads to a decrease in the CMC along with a decrease in $\beta$ as a consequence of an increase in the area per head group of the surfactant ion at the surface of the micelle.[38] For $C_n$PDA, the decrease of $\beta$ is attributed to the flexibility provided by the long alkyl chain in the vicinity of the amides and ether groups, which increases the availability of the amides and ether groups to water, leading to high hydration in the head group region, the increased extent of hydration results in a decrease of $\beta$.[38]

For the availability of the thermodynamic parameters of micellization at various temperatures can give valuable insight into the principles which govern the formation of micelles, so

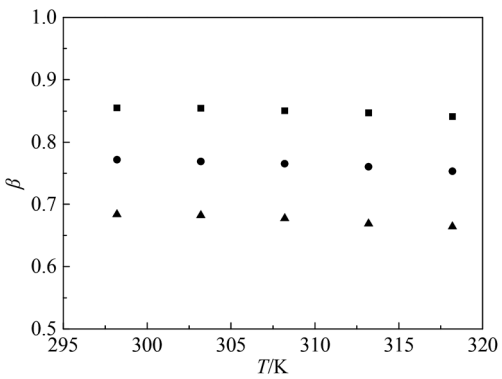


Fig. 5 Plots of the degree of counterion dissociation *versus* the temperature for $C_{12}$PDA (■), $C_{14}$PDA (●) and $C_{16}$PDA (▲).

the parameters of micellization were calculated according to the mass action model using the following equation:[39,40]

$$\Delta G_m^\circ = RT(1 + \beta)\ln X_{CMC} \quad (6)$$

$$\Delta H_m^\circ = \frac{\partial(\Delta G_m^\circ/T)}{\partial(1/T)} \quad (7)$$

$$\Delta S_m^\circ = \frac{\Delta H_m^\circ - \Delta G_m^\circ}{T} \quad (8)$$

where $X_{CMC}$ is the CMC in mole fraction; and $\beta$ is the degree of counter ion binding; following eqn (7), the figures of $\Delta G_m^\circ/T$ *versus* $1/T$ for the solutions of $C_n$PDA were obtained (not given). A second order polynomial was fitted to the data points, and the values of $\Delta H_m^\circ$ were calculated from the slopes of tangential lines at temperatures corresponding to experimental data points. These parameters are listed in Table 3. Plots of Gibbs free energy ($\Delta G_m^\circ$), enthalpy ($\Delta H_m^\circ$), and entropy ($-T\Delta S_m^\circ$) of micellization *versus* the temperature are shown in Fig. 6. It is observed that the values of $\Delta G_m^\circ$ become more negative from −49.0 to −56.9 kJ $mol^{-1}$ with the increase of hydrophobic chain length; and the values of $\Delta G_m^\circ$ for $C_{12}$PDA decreased from −49.0 to −51.7 kJ $mol^{-1}$ with the increase of temperature (Table 3). The negative of $\Delta G_m^\circ$ suggests that $C_n$PDA have great ability to form micelles in aqueous solution; and with the increase of chain length, $C_n$PDA are more likely to form micelles due to the increase of the hydrophobic interactions between the alkyl chains, which is in consistent with the changes of the CMC. It is obviously that the $\Delta H_m^\circ$ value decreases with the rise of temperature for $C_n$PDA with the same alkyl chains length (Fig. 6). In a typical run, the values of $\Delta H_m^\circ$ for $C_{12}$PDA decrease from −1.63 to −15.0 kJ $mol^{-1}$ as the temperature increase from 298.2 to 318.2 K. During the micellization process the variation of enthalpy mainly includes two opposing aspects for the surfactants. One is the removal of water molecules from around the monomeric hydrocarbon chain, and this process is endothermic; another is the transfer of the hydrocarbon chain from the water to the oil-like interior of the micelle, and the transfer process is exothermic.[41] Obviously, the latter is dominant factor as concluded from the experimental results.

The temperature dependence of $\Delta C_{p,m}^\circ$ manifests itself in large negative values of the change in heat capacity ($\Delta C_{p,m}^\circ$),

 

Table 3 Values of thermodynamic parameters from the electric conductivity measurements for CnPDA aqueous solution

| | $T$ (K) | $\Delta G_m^\circ$ (kJ mol$^{-1}$) | $\Delta H_m^\circ$ (kJ mol$^{-1}$) | $-T\Delta S_m^\circ$ (kJ mol$^{-1}$) | $\Delta C_{p,m}^\circ$ (kJ mol$^{-1}$ K$^{-1}$) |
|---|---|---|---|---|---|
| $C_{12}$PDA | 298.2 ± 0.1 | −49.0 ± 0.9 | −1.63 ± 0.03 | −47.3 ± 0.9 | −0.701 ± 0.014 |
| | 303.2 ± 0.1 | −49.7 ± 0.9 | −5.16 ± 0.10 | −44.6 ± 0.9 | −0.679 ± 0.013 |
| | 308.2 ± 0.1 | −50.4 ± 1.0 | −8.56 ± 0.17 | −41.9 ± 0.8 | −0.657 ± 0.013 |
| | 313.2 ± 0.1 | −51.1 ± 1.0 | −11.8 ± 0.2 | −39.2 ± 0.8 | −0.635 ± 0.012 |
| | 318.2 ± 0.1 | −51.7 ± 1.0 | −15.0 ± 0.3 | −36.6 ± 0.7 | −0.613 ± 0.012 |
| $C_{14}$PDA | 298.2 ± 0.1 | −53.0 ± 1.0 | −3.37 ± 0.06 | −49.6 ± 1.0 | −0.810 ± 0.016 |
| | 303.2 ± 0.1 | −53.7 ± 1.0 | −7.68 ± 0.15 | −46.1 ± 0.9 | −0.786 ± 0.015 |
| | 308.2 ± 0.1 | −54.5 ± 1.0 | −11.85 ± 0.23 | −42.6 ± 0.9 | −0.762 ± 0.015 |
| | 313.2 ± 0.1 | −55.1 ± 1.1 | −15.89 ± 0.31 | −39.2 ± 0.8 | −0.738 ± 0.014 |
| | 318.2 ± 0.1 | −55.7 ± 1.1 | −19.81 ± 0.38 | −35.9 ± 0.7 | −0.714 ± 0.014 |
| $C_{16}$PDA | 298.2 ± 0.1 | −56.9 ± 1.1 | −7.85 ± 0.16 | −49.1 ± 1.0 | −0.927 ± 0.019 |
| | 303.2 ± 0.1 | −57.7 ± 1.1 | −12.3 ± 0.2 | −45.4 ± 0.9 | −0.900 ± 0.018 |
| | 308.2 ± 0.1 | −58.4 ± 1.1 | −16.59 ± 0.3 | −41.9 ± 0.9 | −0.873 ± 0.017 |
| | 313.2 ± 0.1 | −59.1 ± 1.1 | −20.76 ± 0.4 | −38.3 ± 0.8 | −0.846 ± 0.017 |
| | 318.2 ± 0.1 | −59.8 ± 1.2 | −24.79 ± 0.5 | −34.9 ± 0.7 | −0.819 ± 0.016 |

which is the unique feature of all processes related to the hydrophobic effect, and it was calculated from eqn (9):[42]

$$\Delta C_{p,m}^\circ = \left(\frac{\partial H_m^\circ}{\partial T}\right)_T \quad (9)$$

As shown in Table 3, that all $\Delta C_{p,m}^\circ$ are negative, which is corresponding with the transfer of the surfactant molecules from their hydrophobically hydrated (ordered) state in the aqueous pseudo-phase to a more labile, water-free micellar interior.[42–44] For $C_{12}$PDA, $C_{14}$PDA, and $C_{16}$PDA, the values of $\Delta C_{p,m}^\circ$ equal −701, −810, and −921 J mol$^{-1}$ K$^{-1}$ with increase of alkyl chain at 298.2 K, respectively, these are more negative than those of $C_n$ABzMe$_2$Cl with the same alkyl chain at 298.2 K, respectively. According to the literature,[45,46] the change in $\Delta C_{p,m}^\circ$ is a linear function of the hydrophobic surface that is not exposed to water in the micelle. For $C_{12}$PDA at 298.2 K, $\Delta C_{p,m}^\circ = -701$ J mol$^{-1}$ K$^{-1}$, indicating that ~21 hydrogen atoms are not in contact with water in the micelle, corresponding to the terminal methyl plus nine methylene groups. Additional, the phenyl group at the end of larger hydrophilic group could fold back toward the micellar core,[42] which may contribute to $\Delta C_{p,m}^\circ$ The results indicate the effect of temperature on micellar property is influenced dominantly by the hydrophobic groups.

Enthalpy–entropy compensation was observed for $C_n$PDA, causing the change in $\Delta G_m^\circ$ to be very small. The value of $\Delta S_m^\circ$ for $C_n$PDA decreased with increasing temperature (Table 3), which could be attributed to the basis of "melting" of the "iceberg structure" of water molecules surrounding hydrophobic moieties.[47] The extensive hydrogen bonding in water gradually breaks down with increasing temperature, causing the importance of the entropic term of hydrophobic hydration to decrease and the dispersion interactions to become increasingly dominant.[48,49] Furthermore, that the entropy term $\Delta TS_m^\circ$ played the dominant role in $\Delta G_m^\circ$ (Fig. 6), in other words, the micellization of $C_n$PDA was entropy-driven in the investigated temperatures range.

## Aggregation number ($N_{agg}$)

The steady-state fluorescence quenching measurements using pyrene as the fluorescent probe and diphenyl ketone as the quencher have been utilized to gain information about $N_{agg}$ of micelles in $C_n$PDA solutions using the following eqn (10):[15]

$$\ln(I_0/I) = \frac{N_{agg}C_q}{(C_t - CMC)} \quad (10)$$

where $C_q$, $C_t$ are the molar concentrations of the quencher, diphenyl ketone, and total concentration of $C_n$PDA, respectively, while $I$ and $I_0$ are the fluorescence intensities of pyrene fluorescence at 376 nm in the presence and absence of quencher, respectively. Pyrene emission spectra *versus* the concentration of quencher for $C_{12}$PDA (A), $C_{14}$PDA (B) and $C_{16}$PDA (C) are given in the ESI.†

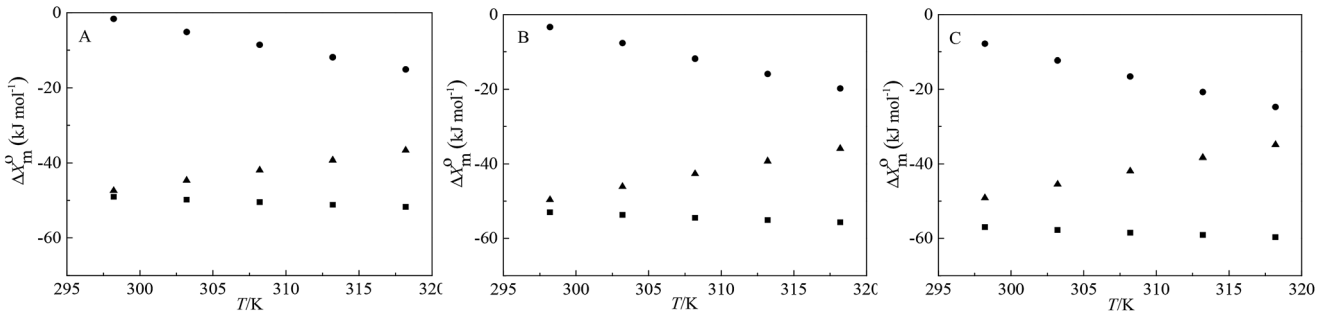


Fig. 6 Variation of $\Delta G_m^\circ$ (■), $\Delta H_m^\circ$ (●), and $-T\Delta S_m^\circ$ (▲) with the temperatures for $C_{12}$PDA (A), $C_{14}$PDA (B) and $C_{16}$PDA (C) in aqueous solutions.

When the concentrations of quencher ranged from 0.01 to 0.25 mmol $L^{-1}$, there is a good linear relationship of $\ln(I_0/I)$ *versus* $C_q$ (Fig. 7). Thus the mean $N_{agg}$ can be determined from the slope of the curve using the CMC value derived from conductivity measurements. The obtained $N_{agg}$ is shown in Table 2. The $N_{agg}$ decreases with the increase of the alkyl chain length and that of the temperature. It implies that the compactness of micelles decreased with the increase in alkyl chain length or the increase of temperature, which led to formation of loose micelles having less number of monomers.[15,32]

### Bactericidal activities

*Staphylococcus aureus*, *Streptococcus*, *Salmonella and Escherichia coli* are the representative of gram-positive bacteria and gram-negative bacteria and widely exists in our living environment, could cause a serious infection of living body. Therefore, it is important to study a kind of effective fungicide. The bactericidal activities of $C_n$PDA and 1227 show good activities against studied strains as shown in Table 4.

It can be found the introduction ether and amide functional groups to the surfactant promoted significantly the bactericidal activity. The bactericidal activity of $C_n$PDA was superior to that of 1227; the bactericidal activities of $C_{14}$PDA is the best for $C_n$PDA, it may be due to the optimum hydrophilic–lipophilic balance of $C_{14}$PDA resulting in the preferential adsorption at the bacterial cell wall to disrupt the bacterial cell membrane.[50]

## Experimental

### Materials and instruments

All of the solvents were of analytical grade and were dried prior to use. 1227 was purchased from Aladdin and used as received; pyrene and diphenyl ketone were purchased from Sigma-Aldrich and used after recrystallization from ethanol; the synthetic procedure and characterization data of the intermediate compound, namely, ethyl phenoxyacetate and *N*′-(2-phenoxyacetyl)-*N*,*N*-dimethylethylenediamine, are provided in ESI.† Millipore water was used in all experiments. FT-IR spectra of the compounds were measured by Nicolet Avatar-370; $^1$H-NMR and $^{13}$C-NMR spectra were recorded on a Bruker AV-600 spectrometer with chemical shifts recorded as ppm in $CDCl_3$, TMS as internal standard; mass spectral analyses were carried out on an Agilent 6310 ESI-Ion Trop Mass spectrometer of Santa Clara, CA, USA; the melting points of $C_n$PDA were determined using a Tektronix X-6 micro melting point apparatus of Beijing Taike, China; surface tension was tested on a K100 Processor Tensiometer, Germany Krüss Company; conductivity was measured on DDS-307A conductivity analyzer with a cell constant of 1 $cm^{-1}$, Shanghai Precision & Scientific Instrument Company; steady-state fluorescence spectra were recorded on Hitachi F-4500 Fluorescence Spectrometer.

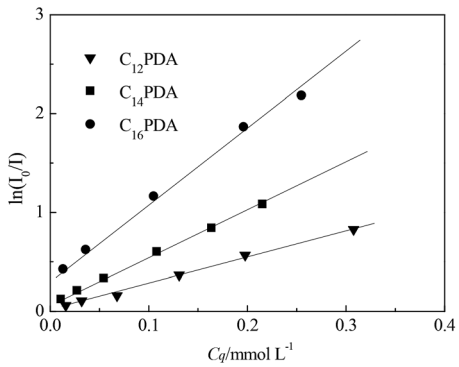


Fig. 7 Variation of $\ln(I_0/I)$ *versus* the concentration of quencher at 298.2 K (the correlation factors of $R^2 > 0.994$).

Table 4 Minimum bactericidal concentration of $C_n$PDA and 1227

| | MBC (μg $mL^{-1}$) | | | |
|---|---|---|---|---|
| Bacterial strains | 1227 | $C_{12}$PDA | $C_{14}$PDA | $C_{16}$PDA |
| *Staphylococcus aureus* | 97.6 | 24.4 | 24.4 | 48.8 |
| *Streptococcus* | 195.3 | 97.6 | 24.4 | 48.8 |
| *Salmonella* | 48.8 | 97.6 | 24.4 | 97.6 |
| *Escherichia coli* | 195.3 | 48.8 | 24.4 | 24.4 |

### Synthesis

The synthetic routes of $C_n$PDA were shown in Scheme 1.

A mixture of *N*-alkyl-2-chloroacetamide and *N*′-(2-phenoxyacetyl)-*N*,*N*-dimethylethylenediamine (mole ratio 1.1 : 1) was dissolved in isopropanol (30 mL), and the solution was refluxed for 18 h. After evaporation of solvent under reduced pressure, the residue was purified three times by recrystallization from chloroform and petroleum ether to give pure product as a white solid. The target products were donated as $C_n$PDA, where *n* represents the carbon number of alkyl chain, $n = 12$, 14 or 16, respectively. All the synthesized surfactants were characterized by $^1$H-NMR, $^{13}$C/DEPT-NMR, ESI-MS and FT-IR, and provided in the ESI.† The spectral data of $C_n$PDA are given below.

**$C_{12}$PDA.** $C_{12}$PDA yield: 82%. M.P.: 89.0–89.5 °C. FT-IR (KBr pellet) $\nu$ $cm^{-1}$: 3444 (N–H, amide), 2917 (–$CH_3$), 2847 (–$CH_2$–), 1683 (C=O, amide), 1061 (Ar-O–R, ether), 890–669 (C–H, aromatic hydrocarbon); $^1$H-NMR (600 MHz, $CDCl_3$): $\delta$ ppm 9.24 (d, $J = 4.8$ Hz, 1H, $C_6H_5OCH_2$ CON*H*), 8.69 (s, 1H, $N(CH_3)_2$-$CH_2CONH$), 6.97–7.30 (m, 5H, $C_6H_5OCH_2CONH$), 4.55 (s, 2H, $C_6H_5OCH_2CONH$), 4.53 (s, 2H, $N(CH_3)_2CH_2CONH$), 3.93 (d, $J =$ 4.8 Hz, 2H, CONH $CH_2CH_2N$), 3.74 (t, $J = 4.8$ Hz, 2H, $CONHCH_2CH_2N$), 3.36 (s, 6H, $N(CH_3)_2CH_2CONH$), 3.21–3.24 (m, 2H, $CONHCH_2CH_2(CH_2)_9CH_3$), 1.53–1.58 (m, 2H, $CONHCH_2CH_2(CH_2)_9CH_3$), 1.24–1.29 (br s, 18H, $CONHCH_2$-$CH_2(CH_2)_9CH_3$), 0.88 (t, $J = 7.2$ Hz, 3H, $CONHCH_2CH_2(CH_2)_9$-$CH_3$); $^{13}$C/DEPT-NMR (150 MHz, $CDCl_3$): $\delta$ ppm 169.83 (–CONH–),

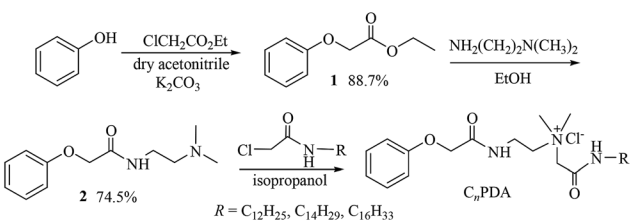


Scheme 1 Synthetic route of $C_n$PDA.

162.47 (–*C*ONH–R), 157.27 (Benzene ring carbon directly attached to –O–$CH_2$–), 129.63 (Benzene ring carbons directly attached to –CH–O–$CH_2$–), 121.97 (Benzene ring carbons directly attached to –CH–CH–O–$CH_2$–), 114.81 (Benzene ring carbons directly attached to –CH–CH–CH–O–$CH_2$–), 66.93 (–O–*C*$H_2$–CONH–), 65.31 (–$N^+$–*C*$H_2$–CONH–), 62.71 (–$CH_2$–*C*$H_2$–$N^+$–), 52.81 (–$N^+$–(*C*$H_3$)$_2$), 39.90 (–CONH–*C*$H_2$–R), 34.08 (–CONH–*C*$H_2$–$CH_2$–$N^+$–), 31.87 (–*C*$H_2CH_2CH_3$), 27.02–29.60 (chain –*C*$H_2$–), 22.64 (–*C*$H_2$–$CH_3$), 14.08 (–*C*$H_3$); ESI-MS (*m*/*z*): $[M - Cl]^+$ 483.89.

**$C_{14}$PDA.** $C_{14}$PDA yield: 74%. M.P.: 92.5–93.5 °C. FT-IR (KBr pellet) $\nu$ $cm^{-1}$: 3444 (N–H, amide), 2913 (–$CH_3$), 2847 (–$CH_2$–), 1683 (C=O, amide), 1078 (Ar-O–R, ether), 882–662 (C–H, aromatic hydrocarbon); $^1$H-NMR (600 MHz, $CDCl_3$): $\delta$ ppm 9.23 (d, $J$ = 4.8 Hz, 1H, $C_6H_5OCH_2CONH$), 8.68 (t, $J$ = 5.1 Hz, 1H, $N(CH_3)_2CH_2CONH$), 6.99–7.29 (m, 5H, $C_6H_5OCH_2CONH$), 4.55 (s, 2H, $C_6H_5OCH_2CONH$), 4.53 (s, 2H, $N(CH_3)_2CH_2CONH$), 3.93 (d, $J$ = 4.8 Hz, 2H, CONH $CH_2CH_2N$), 3.74 (t, $J$ = 5.1 Hz, 2H, $CONHCH_2CH_2N$), 3.36 (s, 6H, $N(CH_3)_2CH_2CONH$), 3.21–3.24 (m, 2H, $CONHCH_2CH_2(CH_2)_{11}CH_3$), 1.53–1.58 (m, 2H, $CONHCH_2CH_2(CH_2)_{11}CH_3$), 1.24–1.29 (br s, 22H, $CONHCH_2CH_2(CH_2)_{11}CH_3$), 0.88 (t, $J$ = 6.9 Hz, 3H, $CONHCH_2CH_2(CH_2)_{11}CH_3$); $^{13}$C/DEPT-NMR (150 MHz, $CDCl_3$): $\delta$ ppm 169.88 (–*C*ONH–), 162.50 (–*C*ONH–R), 157.31 (Benzene ring carbon directly attached to –O–$CH_2$–), 129.67 (Benzene ring carbons directly attached to –CH–O–$CH_2$–), 122.01 (Benzene ring carbons directly attached to –CH–CH–O–$CH_2$–), 114.85 (Benzene ring carbons directly attached to –CH–CH–CH–O–$CH_2$–), 66.96 (–O–*C*$H_2$–CONH–), 65.36 (–$N^+$–*C*$H_2$–CONH–), 62.75 (–$CH_2$–*C*$H_2$–$N^+$–), 52.86 (–$N^+$–(*C*$H_3$)$_2$), 39.95 (–CONH–*C*$H_2$–R), 34.12 (–CONH–*C*$H_2$–$CH_2$–$N^+$–), 31.92 (–*C*$H_2CH_2CH_3$), 27.06–29.70 (chain –*C*$H_2$–), 22.69 (–*C*$H_2$–$CH_3$), 14.13 (–*C*$H_3$); ESI-MS (*m*/*z*): $[M - Cl]^+$ 511.92.

**$C_{16}$PDA.** $C_{16}$PDA yield: 81%. M.P.: 95.2–95.7 °C. FT-IR (KBr pellet) $\nu$ $cm^{-1}$: 3444 (N–H, amide), 2917 (–$CH_3$), 2851 (–$CH_2$–), 1683 (C=O, amide), 1078 (Ar-O–R, ether), 882–665 (C–H, aromatic hydrocarbon), $cm^{-1}$; $^1$H-NMR (600 MHz, $CDCl_3$): $\delta$ ppm 9.26 (s, 1H, $C_6H_5OCH_2CONH$), 8.68 (s, 1H, $N(CH_3)_2CH_2CONH$), 6.99–7.30 (m, 5H, $C_6H_5OCH_2CONH$), 4.54 (s, 2H, $C_6H_5O$ $CH_2$-CONH), 4.53 (s, 2H, $N(CH_3)_2CH_2CONH$), 3.94 (d, $J$ = 2.4 Hz, 2H, $CONHCH_2CH_2N$), 3.73 (s, 2H, $CONHCH_2CH_2N$), 3.36 (s, 6H, $N(CH_3)_2CH_2CONH$), 3.22–3.24 (m, 2H, $CONHCH_2CH_2(CH_2)_{13}CH_3$), 1.54–1.57 (m, 2H, $CONHCH_2CH_2(CH_2)_{13}$ $CH_3$), 1.24–1.29 (br s, 26H, $CONHCH_2CH_2(CH_2)_{13}CH_3$), 0.88 (t, $J$ = 6.9 Hz, 3H, CONH $CH_2CH_2(CH_2)_{13}CH_3$); $^{13}$C/DEPT-NMR (150 MHz, $CDCl_3$): $\delta$ ppm 169.90 (–*C*ONH–), 162.48 (–*C*ONH–R), 157.30 (Benzene ring carbon directly attached to –O–$CH_2$–), 129.67 (Benzene ring carbons directly attached to –CH–O–$CH_2$–), 122.01 (Benzene ring carbons directly attached to –CH–CH–O–$CH_2$–), 114.85 (Benzene ring carbons directly attached to –CH–CH–CH–O–$CH_2$–), 66.96 (–O–*C*$H_2$–CONH–), 65.43 (–$N^+$–*C*$H_2$–CONH–), 62.73 (–$CH_2$–*C*$H_2$–$N^+$–), 52.89 (–$N^+$–(*C*$H_3$)$_2$), 39.96 (–CONH–*C*$H_2$–R), 34.14 (–CONH–*C*$H_2$–$CH_2$–$N^+$–), 31.93 (–*C*$H_2CH_2CH_3$), 27.07–29.71 (chain –*C*$H_2$–), 22.70 (–*C*$H_2$–$CH_3$), 14.13 (–*C*$H_3$); ESI-MS (*m*/*z*): $[M - Cl]^+$ 539.95.

### Measurements

**Equilibrium surface tension.** Surface tension measurements were performed with the ring method at 298.2 ± 0.1 K. Each datum is an average of five individual points, with an accuracy of ±0.1 mN $m^{-1}$. The samples were equilibrated in the measuring vessel for 15 min to minimize the drift due to adsorption kinetics. All the measurements were repeated at least twice.

**Electrical conductivity.** The electrical conductivity method was employed to determine the CMC of $C_n$PDA at the investigated temperatures. Millipore water (specific conductivity of 0.68 μs $cm^{-1}$ at 298.2 K) was used to prepare the solutions for all the surfactants, and the uncertainty of the measurements was within ±2%. For the measurement of CMC, adequate quantities of the concentrated solution were added in order to change the surfactant concentration from concentrations well below the critical micelle concentration to up to at least three times the CMC.

**Steady-state fluorescence.** Pyrene was chosen as the fluorescent probe in the measurement of steady-state fluorescence spectra. The pyrene-surfactant binary solution was dispersed with ultrasound and kept overnight. The emission wavelength ranged from 350 nm to 500 nm, and the excitation wavelength was focused at 335 nm. Excitation and emission slits were fixed at 2.5 and 2.5 nm, respectively. The scan rate was selected at 240 nm $min^{-1}$. The temperature was kept 298.2 K using a water-flow thermostat connected to the cell compartment. The concentration of pyrene was $1.0 \times 10^{-6}$ mol $L^{-1}$ for each solution. In all cases, the concentration of surfactant was used above CMC. A pyrene fluorescence quenching experiment was performed to obtain the aggregation number of the micelles ($N_{agg}$) using diphenyl ketone as the quencher. The pyrene solution was added to the individual and mixed micellar solutions of surfactants. The quencher was added progressively and the intensity was recorded for data analysis.

**Bactericidal activity.** The minimum bactericidal concentrations (MBC) of $C_n$PDA were tested against *Staphylococcus aureus*, *Streptococcus*, *Salmonella* and *Escherichia coli*, by the broth dilution method according to Chinese standard GB15981-1995. Stock solutions were made by serially diluting $C_n$PDA using autoclaved Millipore water. Bacteria to be tested were grown for 6 h in a suitable media and contained ~$10^9$ cfu $mL^{-1}$ (determined by the spread plating method), which was then diluted to $10^5$ cfu $mL^{-1}$ using nutrient media. The concentration of the surfactant with sterilizing rate over 99.9% was picked up as minimum bactericidal concentration (MBC). Each concentration had triplicate values, the whole experiment was done at least twice, and the MBC value was determined by taking the average of triplicate values for each concentration.

## Conclusions

A series of novel cationic surfactants of the *N*-alkylcaramoylmethyl-*N*-[2-(2-phenoxyacetamido)-ethyl]-*N*,*N*-dimethylammonium chloride with amides and ether groups ($C_n$PDA, $n$ = 12, 14, 16) were successfully synthesized. $C_n$PDA possess lower critical micelle concentration and stronger ability to forming micelle in aqueous solution compared with that of $C_n$ABzMe$_2$Cl. The process of micellization of $C_n$PDA is entropy-driven in the temperature range of 298.2 K to 318.2 K. The bactericidal activity of $C_n$PDA is

better than that of 1227 against the studied strains. In conclusion, $C_n$PDA have good advantages both in the surface properties and the antimicrobial activities, and they would serve for potential application as a new sterilizing agent in the future.

## Acknowledgements

This work was supported by the National Natural Science Foundation of China (21176125), the Natural Science Foundation of Heilongjiang Province (B201114, B201314), and the Science Research Project of the Ministry of Education of Heilongjiang Province of China (2012TD012, 12511Z030, JX201210).

## Notes and references

1 L. Pérez, A. Pinazo, R. Pons and M. Infante, *Adv. Colloid Interface Sci.*, 2014, **205**, 134–155.
2 L. Tavano, M. R. Infante, M. A. Riya, A. Pinazo, M. P. Vinardell, M. Mitjans and L. Perez, *Soft Matter*, 2013, **9**, 306–319.
3 Z. Zhao, X. Guo, L. Jia and Y. Liu, *RSC Adv.*, 2014, **4**, 56918–56925.
4 X. Yan, W. Xu, R. Sao, L. Tang and Y. Ji, *Colloids Surf., A*, 2014, **443**, 60–65.
5 L. A. D'Agostino and S. A. Mabury, *Environ. Sci. Technol.*, 2013, **48**, 121–129.
6 P. Bharmoria, M. J. Mehta, I. Pancha and A. Kumar, *J. Phys. Chem. B*, 2014, **118**, 9890–9899.
7 E. Lepeltier, C. Bourgaux and P. Couvreur, *Adv. Drug Delivery Rev.*, 2014, **71**, 86–97.
8 C. Tourne-Peteilh, B. Coasne, M. In, D. Brevet, J. M. Devoisselle, A. Vioux and L. Viau, *Langmuir*, 2014, **30**, 1229–1238.
9 L. Jiang, M. Deng, Y. Wang, D. Liang, Y. Yan and J. Huang, *J. Phys. Chem. B*, 2001, **13**, 7498–7504.
10 H. Fan, B. Li, Y. Yan, J. Huang and W. Kang, *Soft Matter*, 2014, **10**, 4506–4512.
11 V. Chauhan, S. Singh, R. Mishra and G. Kaur, *J. Colloid Interface Sci.*, 2014, **436**, 122–131.
12 V. Chauhan, S. Singh, R. Kamboj, R. Mishra and G. Kaur, *Colloid Polym. Sci.*, 2014, **292**, 467–476.
13 M. T. Garcia, I. Ribosa, L. Perez, A. Manresa and F. Comelles, *Colloids Surf., B*, 2014, **123**, 318–325.
14 J. Hoque, S. Gonuguntla, V. Yarlagadda, D. S. Uppu, P. Kumar and J. Haldar, *Phys. Chem. Chem. Phys.*, 2014, **16**, 11279–11288.
15 R. Kamboj, P. Bharmoria, V. Chauhan, S. Singh, A. Kumar, V. S. Mithu and T. S. Kang, *Langmuir*, 2014, **3**, 9920–9930.
16 V. Chauhan, S. Singh, R. Kamboj, R. Mishra and G. Kaur, *J. Colloid Interface Sci.*, 2014, **417**, 385–395.
17 D. Hu, X. Guo and L. Jia, *J. Surfactants Deterg.*, 2013, **16**, 913–919.
18 Z. Feng, X. Guo, L. Jia and Y. Zhang, *Res. Chem. Intermed.*, 2013, DOI: 10.1007/s11164-013-1492-6.
19 S. Shimizu and O. A. El Seoud, *Langmuir*, 2003, **19**, 238–243.
20 P. H. Mc Cay, A. A. Ocampo-Sosa, G. T. A. Fleming and G. T. Fleming, *Microbiology*, 2010, **156**, 30–38.
21 M. Tandukar, S. Oh, U. Tezel, K. T. Konstantinidis and S. G. Pavlostathis, *Environ. Sci. Technol.*, 2013, **47**, 9730–9738.
22 R. Zana, *Adv. Colloid Interface Sci.*, 2002, **97**, 205–253.
23 F. M. Menger, L. Shi and S. A. A. Rizvi, *J. Am. Chem. Soc.*, 2009, **131**, 10380–10381.
24 P. X. Li, Z. X. Li, H. H. Shen, R. K. Thomas, J. Penfold and J. R. Lu, *Langmuir*, 2013, **29**, 9324–9334.
25 H. Xu, P. X. Li, K. Ma, R. K. Thomas, J. Penfold and J. R. Lu, *Langmuir*, 2013, **29**, 9335–9351.
26 P. X. Li, R. K. Thomas and J. Penfold, *Langmuir*, 2014, **30**, 6739–6747.
27 J. Eastoe, S. Nave, A. Downer, A. Paul, A. Rankin, K. Tribe and J. Penfold, *Langmuir*, 2000, **16**, 4511–4518.
28 W. Qiao, H. Peng, Y. Zhu and H. Cai, *Colloids Surf., A*, 2012, **405**, 45–50.
29 L. Zhi, Q. Li, Y. Li and Y. Song, *Colloids Surf., A*, 2013, **436**, 684–692.
30 I. J. Lin, *J. Phys. Chem.*, 1972, **76**, 2019–2023.
31 N. Li, S. Zhang and L. Zheng, *Phys. Chem. Chem. Phys.*, 2008, **10**, 4375–4377.
32 Q. Zhang, X. Wang, X. Wei and J. Liu, *J. Chem. Eng. Data*, 2013, **58**, 807–813.
33 H. C. Evans, *J. Chem. Soc.*, 1956, 579–586.
34 N. C. Li and W. Brüll, *J. Am. Chem. Soc.*, 1942, **64**, 1635–1637.
35 S. Zhang, J. Yu, J. Wu, W. Tong, Q. Lei and W. J. Fang, *J. Chem. Eng. Data*, 2014, **59**, 2891–2900.
36 J. Tan, D. Ma, S. Feng and C. Zhang, *Colloids Surf., A*, 2013, **417**, 146–153.
37 V. Chauhan, R. Kamboj, S. P. S. Rana, T. Kaur, G. Kaur, S. Singh and T. S. Kang, *J. Colloid Interface Sci.*, 2015, **446**, 263–271.
38 M. J. Rosen, *Surfactants and Interfacial Phenomena*, Wiley, New York, 2nd edn, 1989.
39 R. Zana, *Langmuir*, 1996, **12**, 1208–1211.
40 N. Li, S. Zhang, L. Zheng and T. Inoue, *Langmuir*, 2009, **25**, 10473–10482.
41 M. S. Ramadan, D. F. Evans and R. Lumry, *J. Phys. Chem.*, 1983, **87**, 4538–4543.
42 S. Shimizu, P. A. R. Pires and O. A. El Seoud, *Langmuir*, 2004, **20**, 9551–9559.
43 S. Paula, W. Sues, J. Tuchtenhagen and A. Blume, *J. Phys. Chem.*, 1995, **99**, 11742–11751.
44 A. Chatterjee, S. P. Moulik, S. K. Sanyal, B. K. Mishra and P. M. Puri, *J. Phys. Chem. B*, 2001, **105**, 12823–12831.
45 S. J. Gill and I. Wadsö, *Proc. Natl. Acad. Sci. U. S. A.*, 1976, **73**, 2955–2958.
46 T. Mehrian, A. De Keizer, A. J. Korteweg and J. Lyklema, *Colloids Surf., A*, 1993, **71**, 255–267.
47 H. S. Frank and M. W. Evans, *J. Chem. Phys.*, 1945, **13**, 507–532.
48 C. Tanford, *The Hydrophobic Effect: Formation of Micelles and Biological Membranes*, Wiley, New York, 2nd edn, 1980.
49 W. Blokzijl and J. B. F. N. Engberts, *Angew. Chem., Int. Ed.*, 1993, **32**, 1545–1579.
50 S. Kanjilal, S. Sunitha, P. S. Reddy, K. P. Kumar, U. S. Murty and R. B. Prasad, *Eur. J. Lipid Sci. Technol.*, 2009, **111**, 941–948.

 